Detecting a true quantum pump effect

C. Benjamin[a]

Centre de Physique Theorique, CNRS, UMR 6207-Case 907, Faculté des Sciences de Luminy, 13288 Marseille Cedex 09, France

Abstract. Even though quantum pumping is a very promising field, it has unfortunately not been unambiguously experimentally detected. The reason being that in the experiments the rectification effect overshadows the pumped current. One of the better known ways to detect it is by using the magnetic field symmetry properties of the rectified and pumped currents. The rectified currents are symmetric with respect to magnetic field reversal while the pumped currents do not possess any definite symmetry with respect to field reversal. This feature has been exploited in some recent works. In this work we look beyond this magnetic field symmetry properties and provide examples wherein the nature or magnitudes of the pumped and rectified currents are exactly opposite enabling an effective distinction between the two.

1 Introduction

Quantum pumping is an unique way to transport charge or spin without applying any voltage bias [1,2]. The idea of quantum pumping has been around for a long time beginning with the works of Thouless in reference [3] and Niu in reference [4] and later with the works of Buttiker, Thomas and Pretre in reference [5], Brouwer in reference [6] and Zhou, Spivak and Altshuler in reference [8]. Regrettably the unambiguous detection of this effect has not been possible till date [9,10]. The experiment [11] which was originally thought to be a quantum pumping experiment is now universally accepted as a detection of rectified currents [12]. Although there might have been a pumped current which unfortunately was masked by the rectified currents [9,10,13]. Experimentally, what seems to happen in pumping experiments is that the time dependent parameters may through stray capacitances directly link up with the reservoirs and thus indirectly induce a bias which is the origin of the rectified current [10]. The reason why the urgent detection of a true quantum pump effect is immediately required is because manifold theoretical proposals based on quantum pumping ranging from the use of the quantum pump effect to drive a pure spin current [14,15] to the use of quantum pump effect as a means for quantum computation [16] have come up. With so much at stake an early resolution of this vexed question is not only necessary but also urgently required. This work proposes to answer this question.

Now how to detect pumped and rectified currents if both are present in a single experiment. One of the ways is

to look at the symmetries with respect to magnetic field reversal these currents possess [9,17,18]. To further explain the preceding statement let us start from the definitions of the rectified and pumped currents. The rectified current in a two terminal setup is given by [10]:

$$I_{rect} = \frac{w}{2\pi} R \int_S dX_1 dX_2 \left(C_1 \frac{\partial G}{\partial X_1} - C_2 \frac{\partial G}{\partial X_2} \right). \quad (1)$$

Herein R is the resistance of circuit path and is assumed to be much less than the resistance of the mesoscopic scatterer, while C_1 and C_2 are stray capacitances which link the gates to the reservoirs, X_1 and X_2 are the modulated gate voltages. Finally, G is the Landauer conductance which is just the transmission probability (T) of the mesoscopic scatterer. The pumped current into a specific lead in a two terminal system, is in contrast given as [6]

$$I_{pump} = \frac{e}{\pi} \int_A dX_1 dX_2 \sum_{\beta} \sum_{\alpha \in 1} \text{Im} \left(\frac{\partial S_{\alpha\beta}^*}{dX_1} \frac{\partial S_{\alpha\beta}}{dX_2} \right). \quad (2)$$

In the above equation, $S_{\alpha\beta}$ defines the scattering amplitude (reflection/transmission) of the mesoscopic sample, the periodic variation of the parameters X_1 and X_2 follows a closed path in a parameter space and the pumped current depends on the enclosed area A in (X_1, X_2) parameter space. Initially, the mesoscopic sample is in equilibrium and for it to transport current one needs to simultaneously vary two system parameters $X_1(t) = X_1 + \delta X_1 \sin(wt)$ and $X_2(t) = X_2 + \delta X_2 \sin(wt + \phi)$, herein δX_i defines the amplitude of oscillation of the adiabatically modulated parameters. In the adiabatic quantum pumping regime we consider the system thus is close to equilibrium [7].

[a] e-mail: cbiop@yahoo.com

The essential difference between the rectified currents and the pumped currents are while the former is bound to be symmetric with respect to magnetic field reversal (via, Onsager's symmetry) since the conductance [19] and it's derivatives enter the formula, the pumped currents would have no definite symmetry with respect to magnetic field reversal [17,18] since they in turn depend on the complex scattering amplitudes which have no specific dependence on field reversal unless the scattering system possesses some specific discrete symmetries [18]. The main motivation of this work is to provide examples beyond the distinctive properties the two currents possess with respect to magnetic field reversal.

The examples show that the currents can be easily differentiated, either there natures are so different or their magnitudes are so very different that it enables an easy detection. The three examples provided are: (1) pumped and rectified currents in presence of magnetic barriers; (2) pumped and rectified currents in a normal metal double barrier structure; and finally (3) pumped and rectified currents at a normal metal- charge density wave interface. In example (1) while the pumped currents are cent percent spin polarized the rectified currents are completely unpolarized, in example (2) pumped current is finite while the rectified current is zero, and finally in example (3) the rectified current again is zero while pumped current is finite. Of course these examples are by no means the only examples that can be found there might be numerous other examples wherein the pumped and rectified currents vary in such a distinct fashion apart from of-course the distinction brought out by magnetic field symmetry. In reference [20] the authors consider a three terminal structure with a single normal metal lead with two superconducting leads. The pumped current into the normal metal lead has no definite symmetry with respect to the phase of the order parameter while the conductance is symmetric in phase. In another interesting work [21], the effect of dephasing was considered and it was shown that effect of dephasing on rectification effects is less pronounced than for quantum pumping.

The rectified currents in the adiabatic quantum pumping regime we consider differ from that in the non-linear dc bias regime. In the latter the Onsager symmetry relations are not obeyed [22] while in the former (from Eq. (1)) they are obeyed. Further rectification can also be talked of when a high frequency electromagnetic field is applied to a phase coherent conductor [23]. This case also falls into the non-linear regime.

Our motivation in this work is plain. We provide three examples wherein the distinctive characteristics of the pumped and rectified currents are brought out. The symmetry properties these currents have with respect to magnetic field reversal are not as clear cut as it would seem initially. For example in reference [18] it was pointed out that if the mesoscopic scatterer has some distinct spatial symmetries then the pumped current itself can be symmetric with respect to magnetic field reversal. Our work hopefully will provide a compass which would point into clear blue water between rectified and pumped currents.
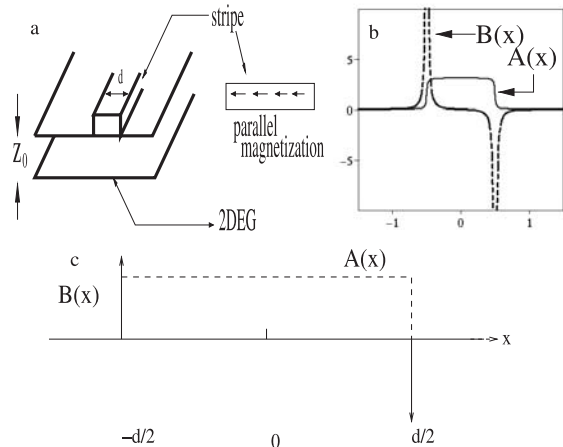

Fig. 1. (a) The device- on top of a 2DEG a parallely magnetized magnetic stripe is placed. (b) The realistic magnetic field profile in a 2DEG along-with the magnetic vector potential for the device represented in (a). (c) The model magnetic field (delta function $B(x)$) profile along with the magnetic vector potential $A(x)$.

2 Examples

In the examples below we look into the weak pumping regime for both the rectified as well as the pumped currents, since we can derive analytical expressions in this regime. The weak pumping regime is defined as one wherein the amplitude of modulation of the parameters is small, i.e., $\delta X_i \ll X_i$. In the weak pumping regime the rectified current reduces to:

$$I_{rect} = I_{rect}^x \left[C_1 \frac{\partial T}{\partial X_1} - C_2 \frac{\partial T}{\partial X_2} \right] \qquad (3)$$

with $I_{rect}^x = we^2 \sin(\phi)\delta X_1 \delta X_2 R/4\pi^2\hbar$. T is the transmission coefficient of the mesoscopic scatterer, and for the special case of capacitances with equal magnitude, i.e., $C_1 = C_2 = C$ one has:

$$I_{rect} = I_{rect}^0 \left[\frac{\partial T}{\partial X_1} - \frac{\partial T}{\partial X_2} \right] \qquad (4)$$

with $I_{rect}^0 = we^2 \sin(\phi)\delta X_1 \delta X_2 RC/4\pi^2\hbar$. Similarly the pumped current into lead α are:

$$I_{pump,\alpha} = I_{pump}^0 \sum_{\beta} \sum_{\alpha \in 1} \text{Im}\left(\frac{\partial S_{\alpha\beta}^*}{dX_1} \frac{\partial S_{\alpha\beta}}{dX_2} \right) \qquad (5)$$

with $I_{pump}^0 = we \sin(\phi)\delta X_1 \delta X_2/2\pi$, w is the frequency of the applied time dependent parameter, ϕ is the phase difference between the parameters and e is the electronic charge.

2.1 Magnetic barrier's

The first example is of pumping and rectification in case of a magnetic barriers. The model of our proposed device is exhibited in Figure 1. It is essentially a 2DEG in

the xy plane with a magnetic field in the z-direction. The magnetic field profile we consider is of delta function type for simplicity, $\mathbf{B} = B_z(x)\hat{z}$ with $B_z(x) = B_0[\delta(x + d/2) - \delta(x - d/2)]$, wherein B_0 gives the strength of the magnetic field and d is the separation between the two δ functions (see Fig. 1c). The above form of the magnetic field is an approximation of the more general form seen when parallely magnetized ferromagnetic materials are lithographically patterned on a 2DEG (Fig. 1b). This approximation is not novel to this work but has been used in a number of works, see reference [21] for further details. Magnetic barrier's can not only be formed by this method but also when a conduction stripe with current driven through it is deposited on a 2DEG, and also when a super-conductor plate is deposited on a 2DEG, see references [24,25] for details. The structure depicted in Figure 1 has been experimentally produced as shown in reference [24]. There are a host of experiments [26] wherein such type of and similar structures are made, discussed and transport measurements carried out.

A 2DEG in the xy plane with a magnetic field pointing in the z direction is described by the Hamiltonian-

$$H = \frac{1}{2m^*}[\mathbf{p} + e\mathbf{A}(x)]^2 + \frac{eg^*}{2m_0}\frac{\sigma\hbar}{2}B_z(x)$$
$$= \frac{1}{2m^*}(p_x{}^2 + [p_y + eA(x)]^2) + \frac{eg^*}{2m_0}\frac{\sigma\hbar}{2}B_z(x) \quad (6)$$

where m^* is the effective mass of the electron, $\mathbf{p}$ is it's momentum, g^* the effective g-factor and m_0 is the free-electron mass in vacuum, $\sigma = +1/-1$ for up/down spin electrons, and $\mathbf{A}(x)$, the magnetic vector potential is given in the landau gauge for the region $-d/2 < x < d/2$ and for incoming electrons from the left by $\mathbf{A}(x) = B_0\hat{y}$, and for electrons incoming from the right by $\mathbf{A}(x) = -B_0\hat{y}$, The magnetic vector potential is zero otherwise. The last term in equation (6) is zero everywhere except at $x = \pm d/2$. For simplicity we introduce dimensionless units, the electron cyclotron frequency $w_c = eB_0/m^*c$, and the magnetic length $l_B = \sqrt{\hbar c/eB_0}$, with B_0 being some typical magnetic field. All the quantities are expressed in dimensionless units: the magnetic field $B_z(x) \rightarrow B_0 B_z(x)$, the magnetic vector potential $\mathbf{A}(\mathbf{x}) \rightarrow B_0 l_B \mathbf{A}(\mathbf{x})$, the coordinate $\mathbf{x} \rightarrow l_b x$ and the energy $E \rightarrow \hbar w_c E(= E_0 E)$.

Since the Hamiltonian as depicted in equation (6) is translation-ally invariant along the y-direction, the total wave-function can be written as $\Psi(x,y) = e^{iqy}\psi(x)$, wherein q is the wave-vector component in the y-direction. Thus one obtains the effective one-dimensional Schroedinger equation-

$$\left[\frac{d^2}{dx^2} - \{A(x) + q\}^2 - \frac{eg^*}{2m_0}\frac{\sigma m^*}{\hbar}B_z(x) \right.$$
$$\left. + \frac{2m^*}{\hbar^2}E\right]\psi(x) = 0. \quad (7)$$

The S-matrix for electron transport across the device can be readily found out by matching the wave functions and as there are δ function potentials there is a discontinuity in the first derivative. The wave functions on the left and right are given by $\psi_1 = (e^{ik_1 x} + re^{-ik_1 x})$ and $\psi_3 = te^{ik_1 x}$, while that in the region $-d/2 < x < d/2$ is $\psi_2 = (ae^{ik_2 x} + be^{-ik_2 x})$. The wave vectors are given by- $k_1 = \sqrt{2E - q^2}$, $k_2 = \sqrt{2E - (q + B_z)^2}$ and for electrons incident from the right, k_2 in the wave-functions is replaced by $k_2' = \sqrt{2E - (q - B_z)^2}$. With this procedure outlined above one can determine all the coefficients of the S-Matrix

$$S_\sigma = \begin{pmatrix} s_{\sigma 11} & s_{\sigma 12} \\ s_{\sigma 21} & s_{\sigma 22} \end{pmatrix} = \begin{pmatrix} r_\sigma & t_\sigma' \\ t_\sigma & r_\sigma' \end{pmatrix}$$

$$r_\sigma = \frac{-i\sin(k_2 d)(k_1^2 - k_2^2 - \lambda^2 - 2i\lambda\sigma k_1)}{D}$$
$$t_\sigma = \frac{2k_1 k_2}{D}, t_\sigma' = \frac{2k_1 k_2'}{D'}$$
$$r_\sigma' = \frac{-i\sin(k_2' d)(k_1^2 - k_2'^2 - \lambda^2 + 2i\lambda\sigma k_1)}{D'}$$

with

$$D = 2k_1 k_2 \cos(k_2 d) - i\sin(k_2 d)(k_1^2 + k_2^2 + \lambda^2),$$
$$D' = 2k_1 k_2' \cos(k_2' d) - i\sin(k_2' d)(k_1^2 + k_2'^2 + \lambda^2),$$
$$\lambda = \frac{g^* B_z}{2}, \ k_1 = \sqrt{2E}, k_2 = \sqrt{2E - (q + B_z)^2}$$

and

$$k_2' = \sqrt{2E - (q - B_z)^2}.$$

One can readily see from the transmission coefficients, there is no spin polarization as $T_{+1} = T_{-1}$. This type of structure has already been studied in reference [14] where it's remarkable pure pumped spin current properties were noticed. In this work we compare and contrast the pumped currents with the rectified currents and show that the rectified currents are completely unpolarized. This provides an unique way to distinguish the two effects. The schematic of the system is exhibited in Figure 1. We in the following consider $q = 0$, and therefore $k_2' = k_2$.

Initially, the device is in equilibrium, and for it to transport current one needs to simultaneously vary two system parameters $X_1(t) = X_1 + \partial X_1 \sin(wt)$ and $X_2(t) = X_2 + \partial X_2 \sin(wt + \phi)$, in our case X_1 is the width d and X_2 the magnetic field B_z given in terms of the magnetization strength $B_0 = M_0 h$, where h is the height and M_0 the magnetization of the ferromagnetic stripe. To invoke pumping in our proposed system we modulate the width $(d = d_0 + d_p \sin(wt))$ and magnetic field strength $(B_z = B_x + B_p \sin(wt + \phi))$. Herein w is the pumping frequency and ϕ is the phase difference between the two modulated parameters. Thus in this adiabatic pumping regime the system is close to equilibrium. The transmission coefficient of this structure which in effect is the Landauer conductance is

$$T = \frac{4k_1^2 k_2^2}{4k_1^2 k_2^2 \cos^2(k_2 d) + (\lambda^2 + k_1^2 + k_2^2)\sin^2(k_2 d)}$$

with,

$$k_1 = \sqrt{2E}, k_2 = \sqrt{2E - B_z^2} \quad \text{and} \quad \lambda_1 = \frac{g^* B_z}{2}. \quad (8)$$

As is self evident, the transmission is completely unpolarized, i.e. $T_\sigma = T_{-\sigma}$. This fact was discovered only in reference [27], two earlier works [28] had mistakenly attributed spin polarizability properties to the device (as depicted in Fig. 1) when a bias is applied. Further because of the fact that spin polarization is absent in presence of a bias, there wont be any spin accumulation [29] either. Hence from equation (4), since the rectified current involves the derivatives of the conductance with respect to the modulated parameters as in equation (4), $X_1 = B_z$ and $X_2 = d$, the rectified current is completely unpolarized. The explicit expression for the rectified and pumped currents are:

$$I_{rect} = I_{rect}^0 \frac{-\sin^2(k_2 d)f' + k_2 \sin(2k_2 d)(f-1)}{T_d'^2},$$

with

$$f = \left[\frac{\lambda_1^2 + k_1^2 + k_2^2}{2k_1 k_2} \right]^2,$$

$$f' = \frac{(2EB_z(4+g^2B) + B_z^3(g^2-4)(1-B_z))}{(64E(2E-B_z^2)^2)}$$

and

$$T_d' = \cos^2(k_2 d) + f\sin^2(k_2 d).$$

In contrast the pumped currents as in reference [14], are given as:

$$I_\sigma = \sigma I_{pump}^0 \frac{2B_z^2 g^* g' k_1^3 k_2^2 \sin(2k_2 d)}{T_d^2},$$

$$I_{sp} = I_{+1} - I_{-1} = I_{pump}^0 \frac{4B_z^2 g^* g' k_1^3 k_2^2 \sin(2k_2 d)}{T_d^2},$$

$$I_{ch} = I_{+1} + I_{-1} = 0,$$

with

$$g' = 1 - \frac{g^{*2}}{4},$$
$$T_d = 4k_1^2 k_2^2 \cos^2(k_2 d) + [4E - g' B_z^2]\sin^2(k_2 d),$$
$$I_{pump}^0 = \frac{ewB_p d_p \sin(\phi)}{2\pi}, \text{and}$$
$$I_{rect}^0 = we^2 \sin(\phi)B_p d_p RC/4\pi^2\hbar.$$

The rectified currents as is evident from the above equations are completely unpolarized, while the pumped currents are completely spin polarized. There is net zero pumped charge current while a finite pure spin current flows. In Figure 2 we show the plots for the pumped currents with the rectified currents plotted in the inset of the figure. The figure for the rectified currents is for equivalent coupling of stray capacitances, but the unpolarized
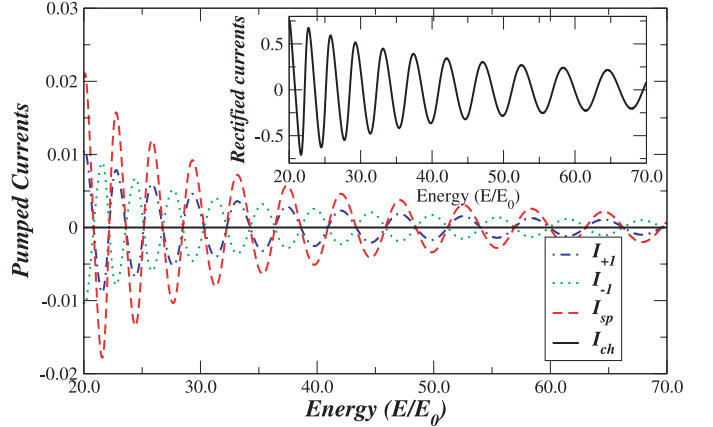

Fig. 2. (Color online) Energy dependence of the pumped current normalized by I_{pump}^0. Spin polarized pumping delivering a finite net spin current along-with zero charge current. The parameters are $B_x = 5.0, d_0 = 5.0, \phi = \pi/2, g^* = 0.44$ and wavevector $q = 0$. In the inset the rectified currents are plotted. The rectified currents normalized by I_{rect}^0 (for same parameters as for pumping) are of-course completely unpolarized.
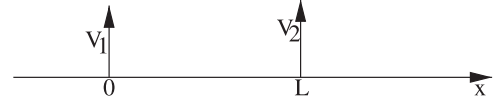

Fig. 3. The double barrier structure. The normal metal double barrier structure is defined via the potential: $V_1\delta(x) + V_2\delta(x-L)$.

nature of the rectified current will be valid as well in case of non-equivalent stray capacitances, since the transmission is completely unpolarized. For $q \neq 0$, as before we have completely unpolarized rectified currents, but in the pumping regime we no longer have pure spin pumped polarized currents but both pumped finite spin and charge currents. Thus the system can again discriminate between pumped and rectified currents but not as as effectively as for the $q = 0$ case.

To conclude the analysis of magnetic barriers, we have shown distinct properties of the rectified and pumped currents. The experimental realization of such type of structures has already been achieved. The only thing one has to add is to adiabatically modulate two independent parameters of our structure (to derive the currents above we have modulated the width of the magnetic barrier and it's strength) to see the distinctive spin polarizability properties the currents possess. To do this one can make a point contact between the ferromagnetic stripe and the 2DEG interface applying an ac gate voltages to this point contact can change the shape of the structure while to change the strength of the barrier one can apply an external time dependent magnetic field to the ferromagnetic stripe.

2.2 Normal metal double barrier structure

In these type of structures pumping has again been studied as in reference [30]. We consider two δ function potentials separated by a length l as in Figure 3. The
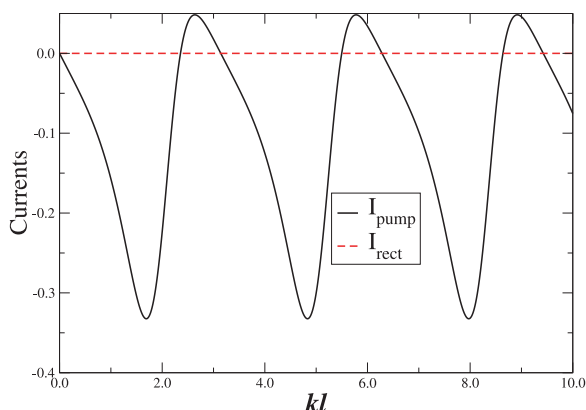
Fig. 4. (Color online) The pumped (normalized by I_{pump}^0) and rectified currents (normalized by I_{rect}^0) for a normal metal double barrier structure as a function of the dimensionless wavevector kl. The strengths of the delta function barriers $z_1 = z_2 = 1.0$.

transmission and reflection amplitudes for such type of structures can be easily calculated by matching the wave-functions at the two interfaces and then by taking into account the jump in the first derivative at the interfaces. The transmission coefficient for this structure is given as:

$$T = \frac{4}{a^2 + b^2} \qquad (9)$$

with,

$$a = z_1 z_2 \sin(kl) + (z_1 + z_2)\cos(kl) - 2\sin(kl),$$
$$b = 2\cos(kl) + (z_1 + z_2)sin(kl), \text{ and } z_i = \frac{mV_i}{\hbar^2 k}.$$

To invoke pumping in these structures we modulate the strengths of the barrier potentials, thus $z_1 = z_{01} + z_p \sin(wt)$, and $z_2 = z_{02} + z_p \sin(wt + \phi)$. One can easily notice from equation (4), that for barriers of equivalent strength $\frac{\partial T}{z_1} = \frac{\partial T}{z_2}$ and the system wont transport any current but a finite pumped current exists. The rectified currents are given by from equation (4),

$$I_{rect} = \frac{-4I_{rect}^0}{(a^2 + b^2)^2}[2z_1 z_2(z_1 - z_2)\sin^2(kl)$$
$$+ (z_1^2 - z_2^2)\sin(2kl) + 2(z_1 - z_2)(\cos(2kl) - 1)]. \quad (10)$$

The rectified current thus by equation (4) is zero for $z_1 = z_2$. In equation (10), $I_{rect}^0 = we^2 \sin(\phi)z_p^2 RC/4\pi^2\hbar$. Of course one must note that this is in addition for equi-potential barriers is valid only if the strengths of the stray capacitances as in equation (4), are also equivalent. Further the pumped currents in the weak pumping regime $z_p \ll z_{0i}, i = 1, 2$, can also be easily derived (from Eq. (5)) and are written below, again for $z_1 = z_2 = z$:

$$I_{pump} = I_{pump}^0 \frac{-8\sin(kl)(z\sin(kl) + \cos(kl))}{(a^2 + b^2)^2}. \qquad (11)$$

Here again a and b are as given in equation (10), and $I_{pump}^0 = we^2 \sin(\phi)z_p^2/\pi$. Thus for barriers of equal magnitude the pumped current is finite while rectified currents
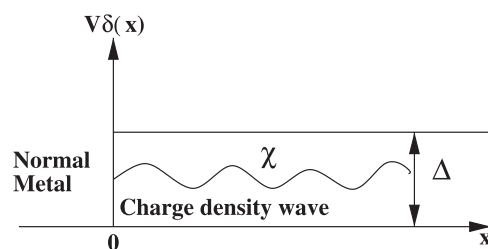

Fig. 5. The normal metal-charge density wave interface. We disregard the proximity effect. Δ denotes the strength of the order parameter of the charge density wave while χ denotes its phase.

are zero. Here we show that the rectified currents are zero in contrast while pumped currents are finite. Of course this result is subject to the condition that the capacitances $C_1 = C_2$. In Figure 3, we plot the rectified currents and pumped currents for such a structure.

The experimental realization of this structure is not at all difficult, since double barrier structures have been ex-perimentally realized for long. The only thing is by having two ac dependent gate voltages to modulate the shape of the double barrier structure such that the coupling to the stray capacitances may be equal. If this condition is real-ized then this very simple structure will be a very good identifier of a genuine quantum pump effect if present. Of course not any structure with equivalent stray capaci-tances will give zero rectified current nor would any device with equi-potential barriers, the most important fact is the equality $dT/dz_1 = dT/dz_2$, which has to satisfied for the absence of rectified currents.

2.3 Normal metal-charge density wave interface

Finally we show that pumping and rectification currents at a normal metal charge density wave interface can also be easily distinguished since the pumped currents are finite while rectified currents are again zero. Since the conduc-tance is effectively zero this result is in fact independent of whether or not $C_1 = C_2$. We consider a normal metal-charge density wave junction with an interface at $x = 0$ as in Figure 5. In the charge density wave region ($x > 0$) the order parameter $\Delta(x) = \Delta e^{i\chi}$ near the interface is not constant but decays smoothly over a finite length of the order of the coherence length [31]. This is the charge den-sity wave proximity effect. In our analysis of the problem we disregard the proximity effect and assume a step func-tion pair potential. The structure we work with is depicted in Figure 5.

A delta function potential $V\delta(x)$ at the interface mod-els the impurity which pins the charge density wave. We also assume the charge density wave and normal metal to be one dimensional and average electron densities are equal. The fermi wave-number k_F and the effective masses are assumed to be equal in the normal metal and charge density wave regions. The scattering matrix of such a junc-tion has been derived earlier in references [33,34]. Here we give the results. The scattering amplitudes of the structure
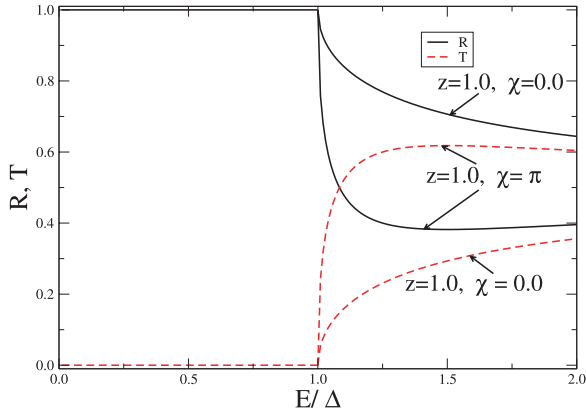
Fig. 6. (Color online) The transmission and reflection probabilities are plotted (parameters are mentioned in the figure). As is evident the transmission is zero in the tunneling regime.

depicted in Figure 5 are given below:

$$r = \frac{-iz(u + ve^{-i\chi}) + ve^{-i\chi}}{(1 + iz)u + izve^{-i\chi}}, \tag{12}$$

$$r' = -\frac{(1 + iz)ve^{i\chi} + izu}{(1 + iz)u + izve^{-i\chi}},$$

$$t = \sqrt{\frac{k}{q}}\frac{1}{(1 + iz)u + izve^{-i\chi}}, \tag{13}$$

$$t' = \sqrt{\frac{q}{k}}\frac{u^2 - v^2}{(1 + iz)u + izve^{-i\chi}} \tag{14}$$

with

$$u^2 = \frac{1}{2}\left(1 + \frac{w}{E}\right), v^2 = \frac{1}{2}\left(1 - \frac{w}{E}\right), \tag{15}$$

in the propagating regime,
and

$$u^2 = \frac{1}{2}\left(1 + \frac{iw'}{E}\right), v^2 = \frac{1}{2}\left(1 - \frac{iw'}{E}\right), \tag{16}$$

in the tunnelling regime.

In the above expressions, $w = \sqrt{E^2 - \Delta^2}$, $w' = i\sqrt{\Delta^2 - E^2}$ and $z = V/\hbar v_F$, with $q = E/\hbar v_F$ and $k = w/\hbar v_F$ in the propagating regime while $k = iw'/\hbar v_F$ in the tunnelling regime, χ is phase of the charge density wave.

The unique thing of such a normal metal-insulator-charge density wave structure is that the macroscopic phase (χ) of the charge density wave appears in the expression for the transmission $|t|^2$ and reflection $|r|^2$ probabilities. This is in sharp contrast to a normal metal-insulator-superconductor structure where the macroscopic phase of the superconductor does not appear in the transmission and reflection probabilities. Here of course we are interested in the distinct characteristics of the rectified current and the pumped current. The unique thing of our structure is that in the tunnelling regime for $E \ll \Delta^2$, the system does not conduct (as $|t|^2 = 0$, see Fig. 6) but pumps a
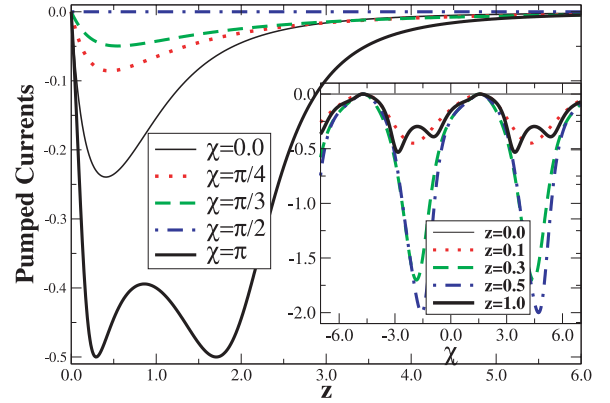

Fig. 7. (Color online) The pumped current into the Charge density wave material at the interface between a normal metal and a charge density wave interface is of course finite in the tunnelling regime ($E \ll \Delta$). In the main panel the pumped currents are as function of the barrier strength z for different values of the phase difference χ, while in the inset the currents are plotted as function of the phase difference χ for different values of the barrier strength z.

finite current as in Figure 7. This is because the transmission probability is zero which can easily be seen also from the above equation, while in the same regime there is a finite pumped current. To invoke pumping in this structure we modulate the strength of the delta function barrier ($z = z_0 + z_p \sin(wt)$) and the phase of the charge density wave order parameter ($\chi = \chi_0 + \chi_p \sin(wt + \phi)$).

In Figure 7, we plot the pumped currents into the charge density wave material for such a structure in the tunneling regime. The transmission and reflection coefficients are also plotted in Figure 6, which bring out the fact that there is no transport in the tunneling regime. The plot clearly brings out the differences as the rectified currents in the tunneling regime are exactly zero while a finite pumped current exists. The expression for the pumped current can also be easily derived in the weak pumping regime $z_p \ll z_0$ and $\chi_p \ll \chi_0$ (see Eq. (4)), and in tunneling regime, i.e., the limit where $E \ll \Delta$-

$$I_{pump}^{CDW} = \frac{2zI_{pump}^0[\sin(\chi) - 1]}{a_z + b_z\cos(\chi) + c_z\sin(\chi) - \cos^2(\chi)[d_z - f_z(\chi)]} \tag{17}$$

with, $I_{pump}^0 = we^2\sin(\phi)z_p\chi_p/\pi$, $a_z = 1 + 8z^4$, $b_z = 4z(1 - 2z)$, $c_z = 4z^2(1 - 2z^2)$, $d_z = 4z^2(z^2 + 2z - 3)$, $f_z(\chi) = 8z^3(\cos(\chi) + \sin(\chi))$.

One can easily see that when the delta function which pins the CDW is absent, i.e., $z = 0$, there is no pumped current. Further when $\chi = \pi/2$ there is again no pumped current. Apart from these two cases the system pumps a finite pumped current for all other values. Browser's formula as in equation (2), was derived for same particles carrying current at both sides of a scatterer. But Brouwer's formulation has been generalized to Normal metal -superconductor junctions [32]. In normal metal-superconductor junctions below the energy gap there cannot be any quasi particle transmission, but there is
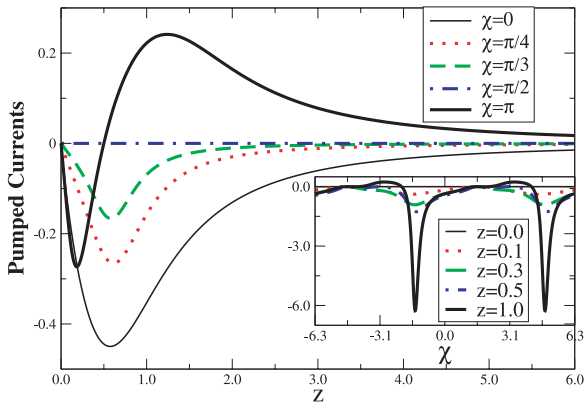
Fig. 8. (Color online) The pumped current into the normal metal lead at the interface between a normal metal and a charge density wave interface is of course finite in the tunneling regime ($E \ll \Delta$). In the main panel the pumped currents are as function of the barrier strength z for different values of the phase difference χ, while in the inset the currents are plotted as function of the phase difference χ for different values of the barrier strength z.

andreev reflection which results in cooper pair transport into superconductor. Something similar happens here below the energy gap. Here there are no cooper pairs, there are instead electron-hole pairs further there is no analog of andreev reflection. What happens when the system is biased is that there is no quasi particle transport into the CDW, since the transmission probability is zero. Since the pumped currents are described by amplitudes reflection and transmission one has a finite pumped current into the CDW. The pumped current into CDW is of-course made of electron-hole pairs.

One can also describe the pumped current into normal metal. One can also distinguish between rectification and pumping via the currents in the normal metal. There is of-course no net rectified current transported into the normal metal lead as whatever is incident at the interface is completed reflected in the tunneling regime ($R = 1$). In-contrast the pumped current is finite and in figure 8 we plot the pumped currents into the normal metal lead. The pumped characteristics can be seen from equation (18), for either $z = 0$ or $\chi = \pi/2$ there is no pumped current similar to the pumped current into the CDW material.

$$I_{pump}^N = \frac{2z I_{pump}^0 [z \sin(2\chi) + \sin(\chi) - 1 - 2z \cos(\chi)]}{4z^4 a(\chi) - 8z^3 b(\chi) - 4z^2 c(\chi) + 4z \cos(\chi) + 1} \tag{18}$$

with, $I_{pump}^0 = w e^2 \sin(\phi) z_p \chi_p / \pi$, $a(\chi) = 2 + 2\sin(\chi) - \sin^2(\chi)$, $b(\chi) = \cos^2(\chi)(\sin(\chi) - \cos(\chi) + 1)$, $c(\chi) = \sin(\chi) + 2\cos(\chi) - 3\cos^2(\chi)$.

The experimental realization of our structure wont be difficult. Mesoscopic charge density wave interfaces have been around for quite awhile now [33]. A metallic gate electrode subject to an oscillating gate voltage is placed on top of the charge density wave material, this arrangement can be effectively used to modulate the phase of the charge density wave [35]. Of course a very similar structure

to that which is envisaged here has been experimentally realized by Adelman et al., in reference [36]. In the experiment of Adelman et al., electric field induced variations of the charge density wave order parameter lead to modulation of the conductance. Further to modulate the interface delta function barrier one can apply an oscillating voltage at the interface. The experimental viability of this structure is of course guaranteed since such type of make-up was theoretically envisaged to provide for a charge density wave ratchet. The only difference will be quantum interference effects dominating and the time dependent voltages being in the adiabatic regime, i.e., at very low temperatures and the system being in the mesoscopic regime.

Finally to conclude this section it should be noted that these three examples may not be unique there might be many other examples of the distinctive nature of the rectified and pumped currents which can be easily and unambiguously detected in experiments.

3 Conclusions

To conclude we have provided three examples in which the pumped and rectified currents are so very distinct. These examples provide an alternative and perhaps better way to distinguish the rectified and pumped currents since these go beyond looking just at the magnetic field symmetry of the currents. The distinctive properties of the rectified and pumped currents will also breakdown if the mesoscopic scatterer has distinct spatial symmetries. In that case looking at the magnetic field symmetry of the currents wont provide the solution. In the first example given above the rectified currents are completely unpolarized while the pumped currents are pure spin polarized, in the second example we have net zero rectified currents for equal strengths of the potential barriers while in example three the rectified currents do not exist at all in the tunneling regime while the system pumps a definite amount of current both in to the charge density wave material and the normal metal lead.

References

1. B. Altshuler, L.I. Glazman, Science **283**, 1864 (1999)
2. G.B. Lubkin, Physics Today **52**, 19 (1999)
3. D.J. Thouless, Phys. Rev. B **27**, 6083 (1983)
4. Q. Niu, Phys. Rev. B **34**, 5093 (1986)
5. M. Buttiker, H. Thomas, A. Pretre, Z. Phys. B: Condens. Matter **94**, 133 (1994)
6. P.W. Brouwer, Phys. Rev. B, **58**, R10135 (1998)
7. M. Moskalets, M. Büttiker, Phys. Rev. B **73**, 125315 (2006)

8. F. Zhou, B.J. Spivak, B. Altshuler, Phys. Rev. Lett. **82**, 608 (1999)

9. M. Moskalets, M. Buttiker, Phys. Rev. B **72**, 035324 (2005); e-print `arXiv:cond-mat/0502106`

10. P.W. Brouwer, Phys. Rev. B **63**, 121303(R) (2001)

11. M. Switkes, C.M. Marcus, K. Campman, A.C. Gossard, Science **283**, 1905 (1999)

12. L. DiCarlo, C.M. Marcus, J.S. Harris, Jr, Phys. Rev. Lett. **91**, 246804 (2003)

13. E.R. Mucciolo, C. Chamon, C.M. Marcus, Phys. Rev. Lett. **89**, 146802 (2002); S.K. Watson, R.M. Potok, C.M. Marcus, V. Umansky, Phys. Rev. Lett. **91**, 258301 (2003)

14. R. Benjamin, C. Benjamin, Phys. Rev. B **69**, 085318 (2004)

15. E.R. Mucciolo, C. Chamon, C.M. Marcus, Phys. Rev. Lett. **89**, 146802 (2002); S.K. Watson, R.M. Potok, C.M. Marcus, V. Umansky, Phys. Rev. Lett. **91**, 258301 (2003); J. Wu, B. Wang, J. Wang, Phys. Rev. B **66**, 205327 (2002); W. Zheng et al., Phys. Rev. B **68**, 113306 (2003); P. Sharma, C. Chamon, Phys. Rev. Lett. **87**, 096401 (2001); T. Aono, Phys. Rev. B **67**, 155303 (2003); M. Governale, F. Taddei, R. Fazio, Phys. Rev. B **68**, 155324 (2003); P. Sharma, P.W. Brouwer, Phys. Rev. Lett. **91**, 166801 (2003); Yadong Wei, L. Wan, B. Wang, J. Wang, Phys. Rev. Lett. **70**, 045418 (2004); K. Yu. Bliokh, Yu. P. Bliokh, Ann. Phys. (NY) e-print `arXiv:quant-ph/0404144`; F. Zhou, Phys. Rev. B **70**, 125321 (2004); A. Brataas, Y. Tserkovnyak, Phys. Rev. Lett. **93**, 087201 (2004); M. Yang, S.-S. Lee, Phys. Rev. B **70**, 195341 (2004); Eran Sela, Yuval Oreg, Phys. Rev. B **71**, 075322 (2005); Cristina Bena, Leon Balents, Phys. Rev. B **70**, 245318 (2004); Y. Tserkovnyak, A. Brataas, G.E.W. Bauer, B.I. Halperin, e-print `arXiv:cond-mat/0409242`

16. P. Samuelson, M. Büttiker, e-print `arXiv:cond-mat/0410581`; C.W.J. Beenakker, M. Titov, B. Trauzettel, e-print `arXiv:cond-mat/0502055`

17. T.A. Shutenko, I. Aleiner, B. Altshuler, Phys. Rev. B **61**, 10366 (2000)

18. I. Aleiner, B. Altshuler, A. Kamenev, Phys. Rev. B **62**, 10373 (2000)

19. M. Buttiker, Phys. Rev. Lett. **57**, 1761 (1986)

20. M. Governale, F. Taddei, R. Fazio, Phys. Rev. B **68**, 155324 (2003)

21. M. Martinez-Mares, C.H. Lewenkopf, E.R. Mucciolo, Phys. Rev. B**69**, 085301 (2004)

22. D. Sanchez, M. Büttiker, Phys. Rev. Lett. **93**, 106802 (2004); B. Spivak, A. Zyuzin, Phys. Rev. Lett. **93**, 226801 (2004); M.L. Polianski, M. Büttiker, Phys. Rev. Lett. **96**, 156804 (2006); D.M. Zumbühl et al., Phys. Rev. Lett. **96**, 206802 (2006)

23. V.I. Fal'ko, Euro. Phys. Lett. **8**, 785 (1989); V.I. Fal'ko, D.E. Khmel'nitskii, Sov. Phys. JETP **68**, 186 (1989)

24. A. Matulis, F.M. Peeters, P. Vasilopoulos, Phys. Rev. Lett. **72**, 1518 (1994); F.M. Peeters, J. De Boeck, in *Handbook of Nanostructured Materials and Nanotechnology*, edited by H.S. Nalwa (Academic, New York, 2000), p. 345

25. M. Lu, L. Zhang, Y. Jin, X. Yan, Eur. Phys. J. B **27**, 565 (2002); F. Zhai, Y. Guo, B.-L. Gu, Phys. Rev. B **66**, 125305 (2002); G. Papp, F.M. Peeters, Appl. Phys. Lett. **79**, 3198 (2001); G. Papp, F.M. Peeters, Appl. Phys. Lett. **78**, 2184 (2001)

26. M.A. McCord, D.D. Awschalom, Appl. Phys. Lett. **57**, 2153 (1990); M.L. Leadbeater et al., J. Appl. Phys. **69**, 4689 (1991); K.M. Krishnan, Appl. Phys. Lett. **61**, 2365 (1992); W. Van Roy et al., J. Magn. Magn. Mater. **121**, 197 (1993); R. Yagi, Y. Iye, J. Phys. Soc. Jpn **62**, 1279 (1993)

27. G. Papp, F.M. Peeters, Appl. Phys. Lett. **79**, 3198 (2001)

28. G. Papp, F.M. Peeters, Appl. Phys. Lett. **78**, 2184 (2001); A. Majumdar, Phys. Rev. B **54**, 11911 (1996)

29. S. Zhang, P.M. Levy, Phys. Rev. B **65**, 052409 (2002)

30. Y. Wei, J. Wang, H. Guo, Phys. Rev. B **62**, 9947 (2000)

31. M.I. Visscher, G.E.W. Bauer, Phys. Rev. B **54**, 2798 (1996)

32. Jian Wang et al., Appl. Phys. Lett. **79**, 3977 (2001), e-print `arXiv:cond-mat/0107077`

33. M.I. Visscher, Ph.D. thesis, Delft University, Netherlands (1998); Masters Thesis, Delft University, Netherlands (1996)

34. Y. Tanaka et al., Solid State Commun. **100**, 37 (1996)

35. M.I. Visscher, Gerrit, E.W. Bauer, Appl. Phys. Lett. **75**, 1007 (1999)

36. T.L. Adelman, S.V. Zatsev-Zotov, R.E. Thorne, Phys. Rev. Lett. **74**, 5264 (1995)